JOURNAL OF APPLIED ELECTROCHEMISTRY 17 (1987) 398–412

Kinetics of the Mn(III)-mediated electrochemical synthesis of sorbic acid precursors from acetic acid and butadiene

SA VAN HO

Corporate Research Laboratories, Monsanto Company, 800 North Lindbergh Boulevard, St. Louis, Missouri 63167, USA

Received 30 September 1985; revised 26 March 1986

The electrochemical synthesis of acetoxyhexenoic acids (precursors of sorbic acid) from acetic acid and butadiene was studied using the redox couple Mn(II)/Mn(III). The kinetics of the homogeneous solution reactions that consumed Mn(III) were studied separately and in conjunction with the simultaneous electrochemical regeneration of Mn(III).

The experimental set-up consisted of a divided electrochemical cell coupled with a stirred tank reactor. Both batch and continuous modes of operation were carried out. In addition to steady-state experiments, transient experiments were also conducted to study the effects of pertinent operating variables on the system performance.

A three-step reaction model was proposed which satisfactorily fits the experimental data.

1. Introduction

In indirect electrochemical synthesis a redox couple, usually inorganic, is used. At the working electrode the oxidizing (or reducing) agent is generated, which then reacts homogeneously with the feedstock either inside or outside the cell to form the desired product. The spent agent is then returned to the cell for regeneration. Thus the agent, termed 'oxygen or hydrogen carrier', can be used over and over again. Examples of this type of approach include the commercial process for the oxidation on anthracene to anthraquinone using the Cr^{3+}/Cr^{6+} redox couple [1], and the oxidation of toluene and chlorobenzene to the corresponding aldehyde using Ce(III)/Ce(IV) [2] or Mn(II)/Mn(III) [3].

In this paper we describe our work on the indirect synthesis of sorbic acid precursors from acetic acid and butadiene using the redox couple Mn(II)/Mn(III).

A possible route to sorbic acid, a food preservative, is shown in the following two-step process:

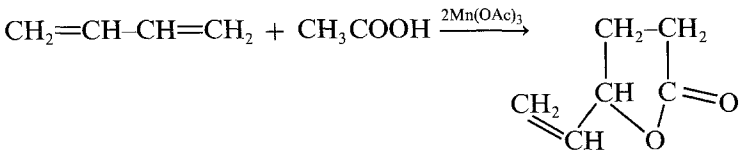

butadiene acetic acid γ-vinyl-γ-butyrolactone (L) (A)

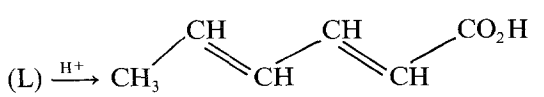

sorbic acid (B)

This chemistry was first described in patents to Nippon Gosei [4, 5]. Note that in step A, 2 moles

0021–891X/87 $03.00 + .12

of $Mn(OAc)_3$ are consumed (converted to $Mn(OAc)_2$) per mole of lactone formed. Since Mn(II) can be oxidized back to Mn(III) electrochemically, the indirect electrochemical synthesis approach discussed above could be used.

The feasibility of generating Mn(III) electrochemically from Mn(II) has been demonstrated by Wagenknecht *et al.* [6] using a parallel plate undivided cell. The electrolysis solution used contained 0.17 M manganous acetate, $Mn(OAc)_2$, and 1.28 M potassium acetate in acetic acid. The cell temperature ranged from 70 to 110° C. The anodic reaction was found to be quite selective for manganous ion, Mn(II), oxidation except at the high current density of 200 mA cm^{-2} when significant amounts of methane, ethane and CO_2 were formed, probably via the oxidation of acetate.

The chemical reaction between Mn(III) and acetic acid with and without the presence of an olefin has been studied by a number of workers. Van der Ploeg and co-workers [7] studied the reaction of manganic acetate in glacial acetic acid with benzene, chlorobenzene or toluene in the 90–110° C temperature range. The main products based on conversion of manganic to manganous acetate (% molar) were found to be acetoxyacetic acid (20%), CO_2 (14.6%), succinic acid (~2%) and methylene diacetate. Methane and methyl acetate were detected in low proportions. According to the authors, these products indicated that the oxidation of acetic acid by Mn(III) yields primarily a C-radical rather than an O-radical:

$$CH_3COOH \xrightarrow[-Mn^{2+},\,-H^+]{Mn^{3+}} \begin{cases} \xrightarrow{\text{side}} CH_3COO^{\cdot} \longrightarrow CH_3^{\cdot} + CO_2 (\longrightarrow \text{Kolbe products}) \\ \xrightarrow{\text{main}} {}^{\cdot}CH_2COOH \end{cases}$$

Subsequent reactions between the radical $^{\cdot}CH_2COOH$ and Mn(III) and with itself lead to the formation of acetoxyacetic acid, succinic acid and CO_2. According to this reaction scheme the formation of acetoxyacetic acid and succinic acid requires 2 moles of Mn(III) each, and CO_2 requires 3 moles of Mn(III). Note, however, that CO_2 generated by the Kolbe reactions only requires 1 mole of Mn(III).

The rate of Mn(III) reduction showed a first order behaviour up to 60–70% conversion only when a molar proportion of $Mn(OAc)_2$ was present. Otherwise deviations were observed and initial rates were appreciably higher. This retarding effect of Mn(II) is believed to be due to the formation of a new complex that contains both Mn(II) and Mn(III).

Hessel [8] found that manganic acetate oxidized acetic anhydride much more readily than acetic acid. The main product was succinic acid (about 60% of the amount of Mn(III) reacted), with traces of acetoxyacetic (~4%). Note the difference in product distribution between this reaction system and the Mn(III)–HOAc. $Mn(OAc)_2$ had a retarding effect on the rate of Mn(III) reaction: the rate decreased threefold as $Mn(OAc)_2$ level was increased from 0 to 20 mM.

Heibe *et al.* [9] found that the addition of potassium acetate at 140° C increased the rate of Mn(III) reduction three to fourfold as well as improving the yield dramatically. These authors postulated that in the presence of acetate ion a new manganic acetate complex, possibly $Mn(OAc)_4^-$, was formed and that this complex decomposed to $^{\cdot}CH_2$–CO_2H radical more rapidly than the neutral complex did.

Klein [10] studied the reaction between $Mn(OAc)_3$ and acetic acid–acetic anhydride mixture. Succinic anhydride and acetoxyacetic acid were found to be the main oxidation products (75% yields of succinic anhydride, 15% acetoxyacetic acid at 120° C). In pure acetic acid, acetoxyacetic acid was the main product.

Bush and Finkbeiner from General Electric [11] and Heiba *et al.* from Mobil [9] studied the reactions between manganic acetate and olefins in acetic acid solution. Both groups found γ-lactones to be the major product. Only traces of CO_2 and methane were formed. Based on this information, these authors suggested that the carboxy-methyl ($^{\cdot}CH_2$–CO_2H) was first formed and then added very fast to the olefin. Acetic anhydride has a dramatic effect on both the rate and yield of the reaction: it speeded up the rate over an order of magnitude and improved the yield from 25 to 72%.

The yields were generally higher when based on the olefins reacted, suggesting the loss of $^{\cdot}CH_2$–CO_2H through reaction pathways that do not involve the olefin, i.e. succinic acid and acetoxyacetic formation [7, 8].

The synthesis of carboxylic acids from α-olefins and acetic anhydride using $Mn(OAc)_3$ was studied by Klein [12] in the temperature range of 100–120° C. With n-octene as the reactant, the major product was decanoic acid; among the major side products were γ-lactones and γ-acetoxyacids. Cu(II) acetate was found to exert a strong effect on the product distribution. According to Klein, the role of Cu(II) was in the efficient trapping of the olefin–$^{\cdot}CH_2$–COOH radical adduct.

From the above literature data it is clear that the reaction between Mn(III) and acetic acid in the presence of an olefin is rather complex and is quite sensitive to the actual composition of the reaction mixture. Therefore, we first studied the kinetics of the Mn(III)–acetic acid–butadiene reaction. The kinetic information was then used to define appropriate conditions for the electrochemical studies, which constituted the major portion of this work.

2. Apparatus and procedure

Batch kinetic experiments involving Mn(III) reactions were carried out in a three-neck 250-ml flask with magnetic stirring. Gases (either N_2 or a mixture of N_2 and butadiene) were introduced through a glass sparger submerged in the solution. Liquid samples were taken at intervals, quenched quickly and later analysed for Mn(III) levels. Concentration of Mn(III) was determined by either spectrophotometry or idometric titration. Spectrophotometry was used for Mn(III) concentrations lower than 5 mM.

The units for carrying out the electrochemical experiments is shown schematically in Fig. 1. Four separate feed tanks were used:

(i) mixed feed containing acetic acid, the electrolyte (KOAc) and the electroactive species ($Mn(OAc)_2$ and $Cu(OAc)_2$),
(ii) pure acetic acid,
(iii) pure acetic anhydride,
(iv) butadiene.

With these separate feeds, any ratio of acetic acid to acetic anhydride in the reaction mixture could be easily obtained. A typical mixed feed contained 0.28 M $Mn(OAc)_2$, 1.76 M KOAc and 30 mM $Cu(OAc)_2$ in acetic acid.

A divided electrochemical cell was used, with the anode compartment connected to the reactor and the cathode side connected to the catholyte tank. The two compartments of the cell were separated by a cation exchange Nafion membrane. The cell frame consisted of two polypropylene blocks with built-in channels for flow distribution. Neoprene gaskets were used between the membrane and the polypropylene blocks. Polypropylene turbulence promoter was used on both sides of the membrane, between the membrane and an electrode, to promote good mass transfer as well as to keep the membrane in place. Electrical connections were made by screwing a metal rod into the back of the electrode. Either stainless steel or graphite plate was used for the cathode. When carbon felt was used as the anode, the felt rested on a graphite backplate to which the electrical connection was made. A platinum wire was also put between the graphite plate and the felt to obtain good electrical contact. The dimensions of both anode and cathode were 4 cm by 30 cm. Two stainless steel metal plates with bolts were used to secure the polypropylene blocks.

The reactor was heated with band heaters and was temperature-controlled. Gas–liquid mixing in the reactor was achieved by circulating the overhead gas through a glass sparger that was submerged in the liquid. The liquid was circulated through the anode compartment by a pump.

The acetic acid stream was fed to the cathode tank, while the other three feed streams were fed to the reactor. The catholyte contained acetic acid and KOAc. During electrolysis, hydrogen gas was produced at the cathode, and K^+ plus HOAc was transported through the membrane from the

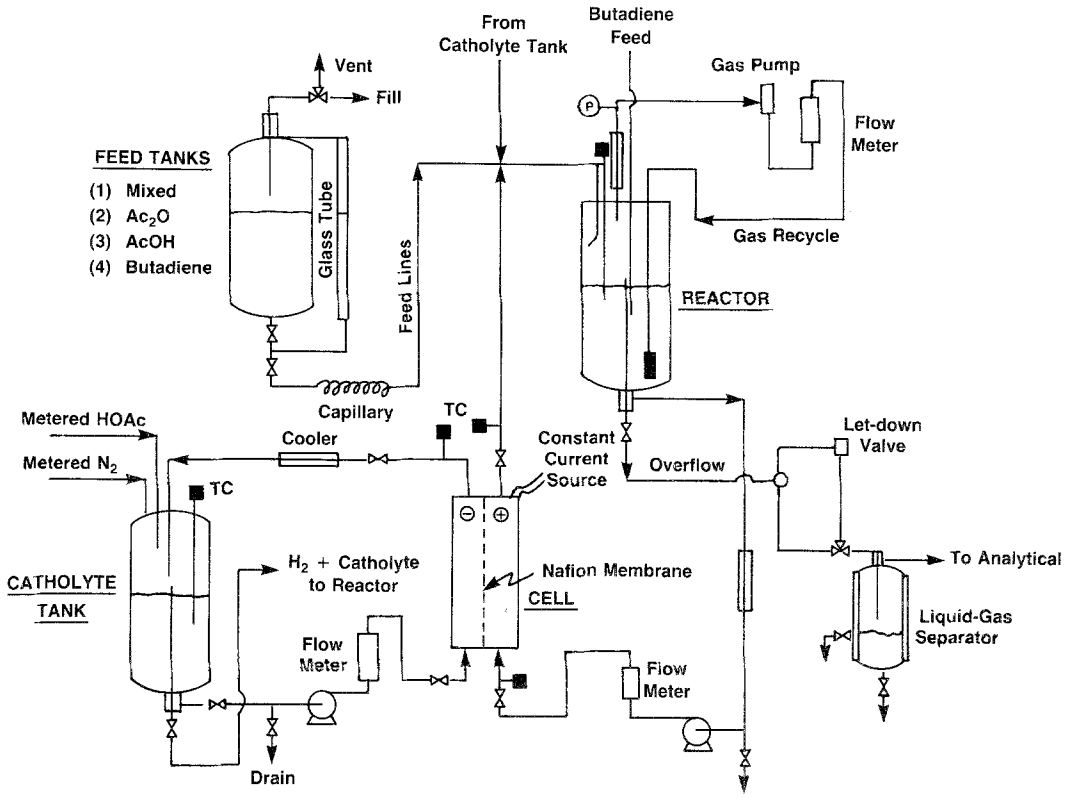

Fig. 1. Schematic diagram for the continuous electrolysis unit.

anode to the cathode side. The fed acetic acid would be mixed with the catholyte and the excess liquid was forced by hydrogen through an overflow tube to the reactor + anode side. With this set-up the potassium salt was brought back to the reactor and the KOAc concentration in the catholyte was maintained at a constant value during the electrolysis.

A known amount of N_2 gas (20 cm^3 STP per minute) was also constantly fed to the catholyte tank. This nitrogen served both as a driving force for bringing the excess catholyte to the reactor side and as an internal standard for GC gas analysis.

The overflow from the reactor was brought to a jacketed gas–liquid separator where the liquid was collected at the bottom, and the gas proceeded to an on-line GC system for gas analysis. The volume of the reactor (up to the overflow tube) + anode compartment was about 440 ml.

For pressure operations the cell was housed in a stainless steel bell jar. The jar was hooked up such that it was pressurized along with the reactor system. The pressure differential was only about 3 psi higher in the cell, which helped minimize leakage problems.

All the parts that were in contact with solution containing Mn(III) (e.g. reactor, flow meter, tubing, etc.) were made from zirconium to avoid corosion problems. Some other suitable materials of construction are Teflon, polypropylene and glass.

Analysis of acetoxyhexenoic acids (found to be the major product in this work as discussed in the following section) in the liquid stream involved preparing the trimethysilyl derivatives for gas chromatography. A 10% SE52/100-120 mesh high performance chromosorb W-column was used with the oven temperature programmed from 80 to 240° C at 10° C per minute. This method also quantified γ-vinyl-γ-butyrolactone and sorbic acid. Butadiene concentration in the electrolysis solution was measured by gas chromatography with benzophenone as the internal standard.

The on-line GC system for gaseous analysis consisted of two separate gas chromatographs. The

following gases were quantified:

*GC 1: N_2, 1-butene, *cis*-2-butene, *trans*-2-butene, 1,3-butadiene, acetic anhydride and acetic acid.

*GC 2: H_2, N_2, CH_4, CO, CO_2, ethylene and ethane.

3. Results and discussion

3.1. *Batch chemical experiments*

The kinetics of the solution reactions that involve Mn(III) were first studied to obtain a basis for assessing their role in the actual electrolyses. In order to separate the effects of different components, the rate of Mn(III) disappearance was measured in acetic acid (HOAc) alone, or in mixtures of HOAc and acetic anhydride (Ac_2O) with or without Cu(II), butadiene and $Mn(OAc)_2$. It was found that practically every compound present had an effect on the rate of Mn(III) reduction.

The following important kinetic information was obtained:

(i) Acetic anhydride clearly exerted a remarkable accelerating effect on the rate of Mn(III) reduction: the rate was an order of magnitude faster in a mixture of HOAc–Ac_2O than in HOAc. This phenomenon was also observed by Hessel [8] and Bush and Finkbeiner [11]. The rate was found to be first order with respect to Mn(III) concentration. The rate was also linearly proportional to the level of acetic anhydride (Fig. 2). Thus it seems that in HOAc–Ac_2O mixture Mn(III) preferably reacts with Ac_2O first.

(ii) The presence of Mn(II) adversely affects the rate of Mn(III) reduction. This inhibiting effect becomes less pronounced at Mn(II) concentrations above 80 mM. Fig. 3 shows that data for Mn(II) concentration ranging from 0 to 120 mM. The reaction was first order with respect to Mn(III) concentration both with and without butadiene. According to van der Ploeg *et al.* [7] a possible explanation for this inhibiting effect of Mn(II) is that $Mn(OAc)_2$ and $Mn(OAc)_3$ form a complex in

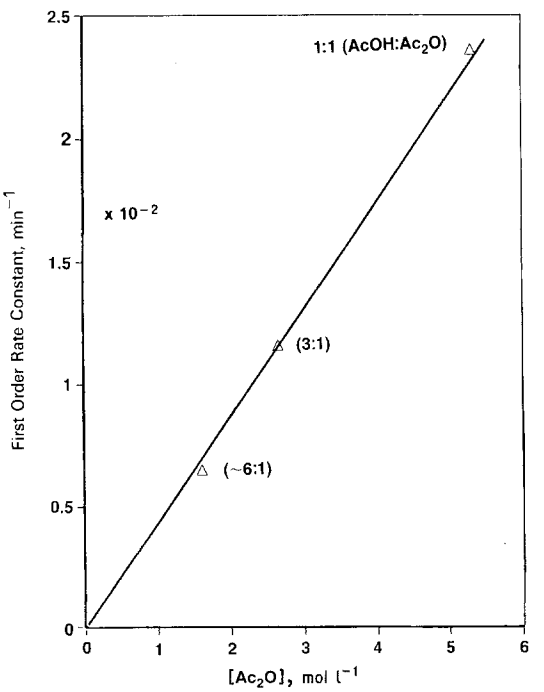

Fig. 2. Effect of acetic anhydride concentration on the rate of Mn(III) reduction. Reaction mixture: 5 mM $Cu(OAc)_2$, 10 mM $Mn(OAc)_3$, 0.76 M KOAc and butadiene at 72° C.

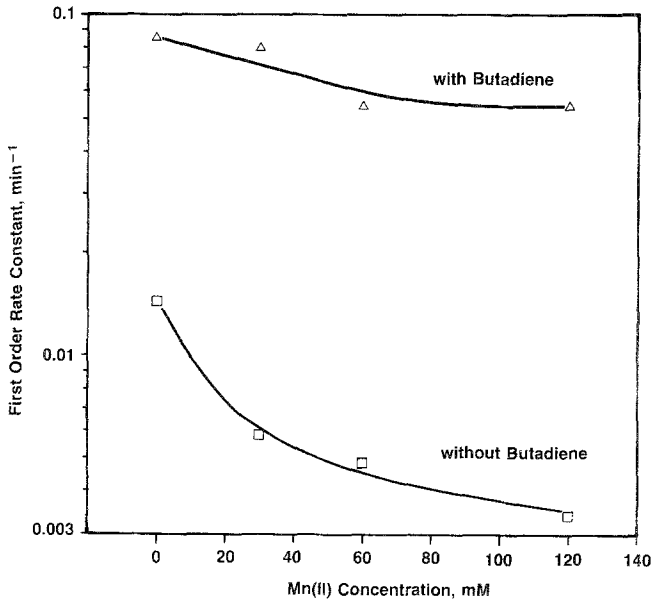

Fig. 3. Inhibiting effect of Mn(II) on Mn(III) reduction. Reaction mixture: 9.6 M HOAc, 4 M Ac_2O, 1 M KOAc, and 0.55 M LiOAc at 92° C.

solution and that this complex is less reactive than $Mn(OAc)_3$ alone. Note in Fig. 3 that the presence of butadiene enhanced the rate of Mn(III) reduction by an order of magnitude.

(iii) The presence of Cu(II) increased the rate of Mn(III) reduction only slightly. For example, the rate increased about 20% when 5 mM $Cu(OAc)_2$ was added to a HOA–Ac_2O–butadiene mixture. Doubling the Cu(II) level to 10 mM had no further effect on the rate.

(iv) The effect of temperature on the rate of Mn(III) reduction in various reaction mixtures was determined for the temperature range of 60–105° C. The activation energy ranged from 17 to 29 kcal g mol^{-1} depending upon the electrolyte used as well as whether butadiene and acetic anhydride were present or not.

(v) The reaction of butadiene, acetic acid and stoichiometric amounts of manganic acetate as reported (150° C) gave lactone yields of 30–40%. However, in the presence of acetic anhydride the major products were found to be the following mixture of acetoxyhexenoic acids (AA) instead of lactone:

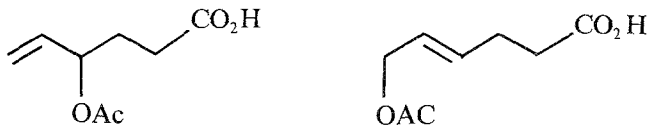

Milder temperatures were used (< 110° C) and AA yields were much higher. The effects of operating conditions on AA production are reported in the next section in which experiments were carried out with *in situ* electrochemical regeneration of Mn(III) along with the solution chemical reactions. The effect of acetic anhydride of the product distribution from the reaction mechanism standpoint is discussed in Section 4.

Acetoxyhexenoic acids can be catalytically converted to sorbic acid either directly or through lactone. This will be the topic of a future publication.

3.2. *Electrochemical experiments*

Values for the current efficiency reported in this section are calculated on the basis that formation of 1 mole of either lactone or acetoxyhexenoic acid (AA) requires 2 moles of Mn(III), which is equivalent to 2 Faradays being charged to the electrochemical cell.

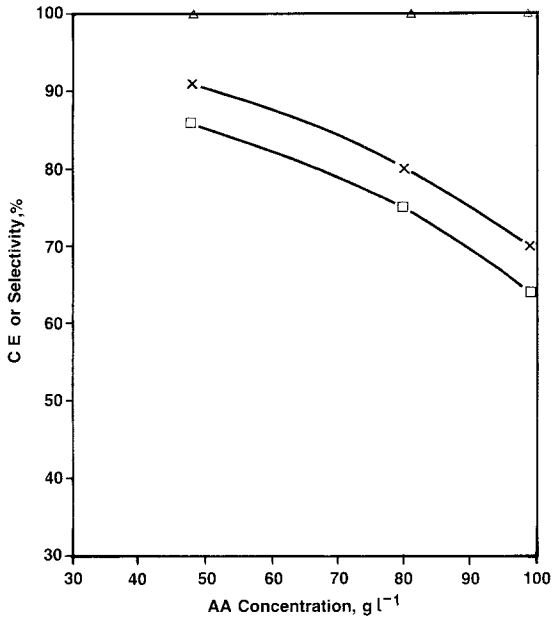

Fig. 4. Current efficiency for acetoxy acid and hydrogen formation — batch data. Electrolysis conditions: apparent current density, 15 mA cm^{-2}, temperature, 100° C. Δ, H_2 current efficiency; □, AA current efficiency; x, butadiene selectivity.

3.2.1. Batch experiments. Batch runs using either graphite or carbon felt as the anode material were carried out. Either stainless steel or graphite could be used for the cathode. A typical anolyte composition used was 3 HOAc to 1 Ac_2O (volume), 70 mM $Cu(OAc)_2$, 200 mM $Mn(OAc)_2$ and 1.5 M KOAc. The reactor temperature was 100° C and the cell temperature was 93°. Under the above conditions the major products were found to be the two isomers of acetoxy hexenoic acids (AA), the minor products being γ-vinyl-γ-butyrolactone and some unidentified high boilers. The results for the batch runs are shown in Fig. 4. It can be seen that the current efficiency for AA was quite high at low AA concentration in the reaction mixture (~90% at 40 g l^{-1} of AA). The current efficiency of AA, however, dropped consistently as its concentration in the reaction mixture built up. This loss in current efficiency was not due to the Kolbe reactions (anodic oxidation of acetic acid) because CO_2, a product of this reaction, constituted less than 1% of the overall current efficiency throughout the run.

The selectivity of butadiene to AA, which is not affected by side electrode reactions that do not involve AA, also followed the shape of the AA current efficiency curve. This is a good indication that the efficiency loss was probably due to the loss of AA itself through further reactions. The only cathode reaction seems to be the formation of H_2 and this was very efficient (100% current efficiency).

The positive graphite plate was found to be partially covered with a black material after a run, indicating that electrode fouling may have occurred. The carbon felt seemed to be more stable, probably due to its high surface area which resulted in a lower actual current density for the same current passed.

3.2.2. Continuous experiments. From a process standpoint, continuous operation is more preferable than batch operation. For this system, there is also a severe problem with batch operation. During the electrolysis potassium ion (K^+) was continually transported with HOAc through the membrane, causing the salt concentration in the catholyte to increase with time. At the same time the anolyte was being depleted of the electrolyte. As a consequence, the cell voltage went up. With continuous operation, this problem was eliminated. Operational procedure for continuous experiments is detailed in the Apparatus and procedure section.

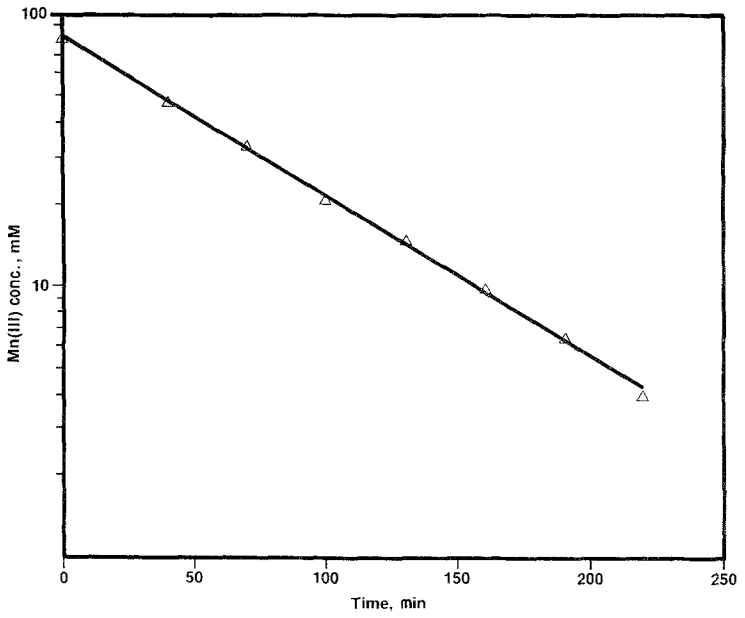

Fig. 5. CSTR fit for a step decrease in Mn(III) concentration.

3.2.2.1. Transient experiments.

(i) Tracer tests – no chemical reaction. Transient experiments were carried out with Mn(III) as the tracer to characterize the reactor system. Using Mn(III) as the tracer was very convenient because a step increase was obtained by just turning the cell current on to generate Mn(III) *in situ*. Turning off the current with the liquid feed on constituted a step-decrease experiment. In these tracer tests the temperature of the cell and the reactor was deliberately kept low ($\sim 50°$ C) and no acetic anhydride was used so that the chemical reactions consuming Mn(III) were completely insignificant. Both step increase and step decrease data fit the behaviour of a perfectly mixed reactor (CSTR) very well. Fig. 5 shows the fit for the step-decrease experiment. In the step increase experiment, the current efficiency for Mn(III) generation could be calculated from the Mn(III) concentration in the effluent when the system had reached steady state. The current efficiency was found to be over 95%.

(ii) Under reaction conditions. The transient responses for Mn(III) and AA in an actual electrolysis experiment are shown in Fig. 6. Note that it took between three and four residence times for the

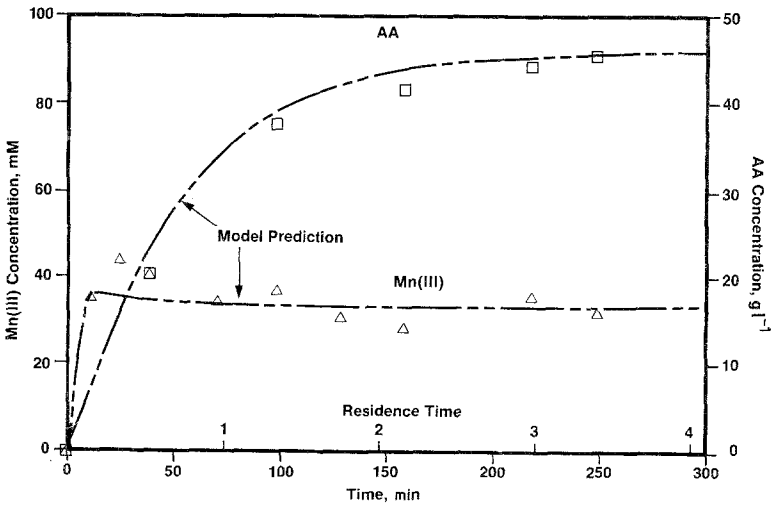

Fig. 6. Transient responses for AA synthesis – comparison between data and model prediction. □, AA; △, Mn(III). Dashed curve: prediction by the three-step model. Electrolysis conditions: temperature = 100° C; apparent current density = 104 mA cm^{-2}; reaction solution starting with 10 mM Cu(II), 100 mM Mn(II) and 0.6 M KOAc.

system to reach steady state in accordance with CSTR behaviour. It is interesting that the Mn(III) concentration curve went through a maximum. This suggests the existence of a side reaction that consumes Mn(III) as AA concentration builds up. As will be seen later, the pronounced effect of this behaviour was manifested in the steady-state data.

3.2.2.2. Steady-state data – effects of operating variables.

(i) Cupric acetate improved the synthesis efficiency of AA. For example, the current efficiency for AA dropped from 75 to 44% when Cu(II) was removed from the reaction mixture. The beneficial effect of Cu(II) was probably owing to its efficient oxidation of the radical adduct (step 3 in the reaction mechanism, Section 4).

(ii) Increasing the acetic anhydride level significantly speeded up the chemical rates; AA current efficiency was also improved. The gain in AA current efficiency, however, became insignificant for a Ac_2O to AcOH volume ratio higher than 0.5 (Fig. 7). Notice in this figure that as the Ac_2O level was increased the steady-state Mn^{3+} level decreased, which is consistent with the kinetic finding that the rate of Mn^{3+} disappearance is proportional to Ac_2O level. With a sufficient amount of acetic anhydride in the electrolysis solution, acetoxyhexenoic acids (both branched and linear isomers) were always the major reaction products. Only a small amount of γ-vinyl-γ-butyrolactone was detected. As concentration of acetic anhydride was lowered, lactone became the major product; the overall current efficiency was, however, significantly reduced.

(iii) The effect of Mn^{3+} concentration on AA current efficiency was studied by varying both current density and feed rate. In these experiments the current density was doubled (from 52 to 104 mA cm^{-2}) to obtain higher steady-state Mn^{3+} concentration in the reactor; at the same time the feed rate was doubled so that AA concentration in the reaction mixture remained more or less constant. The steady-state Mn^{3+} concentration was found to increase from 10 to 36 mM, but no change in AA current efficiency was observed.

(iv) A series of runs was carried out to explore the effect of increasing current density. The results are shown in Table 1. As can be seen, at an apparent current density of 26 mA cm^{-2} and 2.5 wt % AA, the AA current efficiency was 85% and butadiene selectivity was 95%. Increasing the current density but keeping the feed rate constant caused a decline in both AA current efficiency and butadiene selectivity. At 78 mA cm^{-2} the current efficiency as well as butadiene selectivity were only 65%. Current efficiency for CO_2 remained low at $< 1\%$, indicating that current efficiency loss was

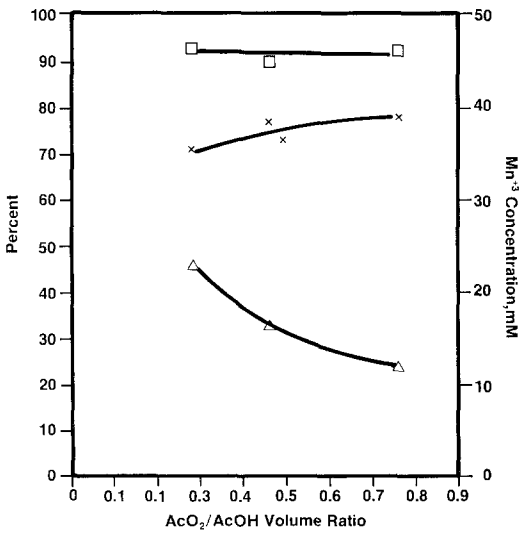

Fig. 7. Effect of acetic anhydride level on the continuous electrolysis results. Electrolysis conditions: apparent current density = 52 mA cm^{-2}; cell temperature = 95° C, reactor temperature = 104° C; AA payload = 4.4 wt %. Reaction mixture is similar to that of Fig. 6. □, Butadiene selectivity; ×, AA current efficiency; △, Mn^{3+} concentration.

Table 1. Effects of current density

Run	*Current density* ($mA\,cm^{-2}$)	*Temperature* (°C)		*Concentration* (mM)		*AA current efficiency* (%)	*Butadiene selectivity*	*AA payload* (wt%)	H_2 *evolution* (%)
		Cell	*Reactor*	Mn^{3+}	*Butadiene*				
1	26	93.5	100	7.5	–	85	95	2.5	97
2	32.5	95	100	9	74	76	92	3.4	96
3	52	94	104	17	110	76	89	4.4	94
4	65	94	103.5	18	74	70	76.5	5.1	92
5	78	96	105	22	–	66	65	5.5	91
6[a]	104	102	104	39.5	80	73.6	72	4.6	87
7[b]	104	106	109	27.5	–	55	64	8.0	92

[a] Liquid feed rate for this run was 5.8 ml min^{-1} compared to 3 ml min^{-1} for the rest.
[b] 4 wt% AA in feed stream for this run.

Table 2. Effects of pressure and temperature. Ac_2O to AcOH ratio = 0.3–0.33

Pressure (atm)	*Temperature (°C)*		*Concentration (mM)*		*Current efficiency (%)*		*Butadiene selectivity (%)*
	Reactor	*Cell*	Mn^{3+}	*Butadiene*	*AA + Lactone*	H_2	
1.0	104.5	102	39.5	86	75	87	72
3.86	106	100	42.5	247	77	85	73
3.86	120	110	11.0	277	71	87	60

not due to the Kolbe reaction. The loss in current efficiency at high current density was likely due to the resulting increase in AA concentration. An experiment with the feed containing about 4 wt % AA to simulate the high current density run (run 7 in Table 1) confirmed this. The steady-state AA level for this run was 8 wt % and the corresponding current efficiency was only 55% compared to 74% for the same run but without AA in the feed. As will be shown later, further oxidation of AA by Mn(III) is the cause for the observed decline in current efficiency.

(v) The total pressure and temperature of the system directly affected the concentration of butadiene in the solution. Table 2 shows the results for both atmosphere and higher pressure runs at 104 mA cm^{-2} and with ~4.6 wt % AA. As can be seen, other than the difference in pressure, similar operating conditions resulted in comparable AA current efficiency and butadiene selectivity, even though butadiene concentration in the reaction solution at 3.8 atm was almost three times higher than that at atmospheric pressure. Also, the steady-state Mn(III) concentration, an indicator of the rate of the solution reactions, hardly changed despite the threefold increase in butadiene concentration in the high pressure run. Thus the rates were insensitive to butadiene concentration in this range and pressure operation was not necessary for increasing chemical rates. Raising the reaction temperature seemed to promote more lactone formation in the product. Around 100° C lactone constituted less than 10 mol % of the electrolysis product whereas at 130° C it increased to about 30%.

3.3. *Comparison of batch and continuous data — cause for AA loss*

Results from both batch and continuous experiments show that AA current efficiency dropped drastically as payload increased, indicating that AA was not stable in the reaction medium. At the same final payload the continuous current efficiency was, however, consistently lower than the batch value.

The main difference between those two modes of operation is that in the continuous mode, AA concentration was constant at its steady-state value whereas AA in the batch mode started out at zero, then increased with time. The instability of AA could account for the noted deviation in current efficiency between the two modes of operation.

In a Mn(III)-free environment, AA is quite stable. Heating for 3 h at 150° C only destroyed about 8% of the initial acetoxyacids. The reaction between Mn^{3+} and AA was checked experimentally by comparing the rates of Mn^{3+} disappearance in reaction mixture with and without the presence of acetoxyacids. It was found that the presence of acetoxyacids, without butadiene, speeded up the rate of Mn^{3+} disappearance significantly. At 80° C and with the solution mixture consisting of 2 AcOH to 1 Ac_2O, 1.5 M KOAc and 17 mM Mn^{3+}, adding AA (180 mM) increased the rate of the Mn^{3+} consumption several fold. The amount of Mn^{3+} disappearing was comparable to the amount of AA consumed. This AA–Mn^{3+} reaction is first order with respect to Mn^{3+} concentration. Thus, from a kinetic standpoint the following may represent what was happening in the reaction

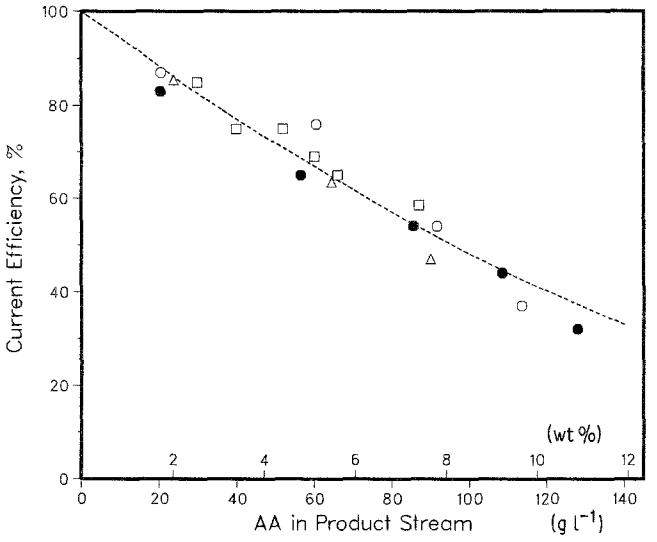

Fig. 8. AA current efficiency versus payload – comparison of batch data and continuous data, and experimental data and model prediction. Filled symbols, batch data; open symbols, continuous data; dashed line, prediction by the three-step model.

mixture:

$$Mn^{3+} + \begin{cases} AcOH\text{–}Ac_2O \\ Cu^{2+} \\ \text{butadiene} \end{cases} \longrightarrow \quad AA \qquad \text{(a)}$$

$$Mn^{3+} + AA \longrightarrow \text{High boilers} \qquad \text{(b)}$$

The severity of reaction (b) depends on the level of AA, which is consistent with the observed drop in AA current efficiency at high payloads. Since AA was being continuously consumed through its reaction with Mn(III) during electrolysis, comparison between batch and continuous data ought to be done at comparable AA concentrations. One approach is to average the concentration of AA over the operating time interval for the batch case. When this was carried out, excellent agreement between the two modes of operation was obtained (Fig. 8).

4. Reaction mechanism and modelling

4.1. *Mechanism*

The following mechanism is proposed in general agreement with experimental data.

Electrode reactions:

$$\text{Anode:} \quad 2Mn(II) \xrightarrow{-2e} 2Mn(III)$$

$$\text{Cathode:} \quad 2H^+ + 2e \longrightarrow H_2 \text{ gas}$$

Solution reactions:

$$Mn(III) + CH_3\text{–}COOR \xrightarrow{1} {}^{\cdot}CH_2\text{–}COOR + H^+ + Mn(II)$$

$${}^{\cdot}CH_2\text{–}COOR + \underset{\text{(Butadiene)}}{\text{ 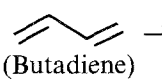 }} \xrightarrow{2} \begin{cases} \text{ 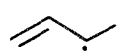 } - CH_2\text{–}COOR \\ \text{ 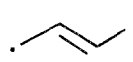 } - CH_2\text{–}COOR \end{cases}$$

This addition of butadiene to the radical is a very fast reaction (see Section 3.1).

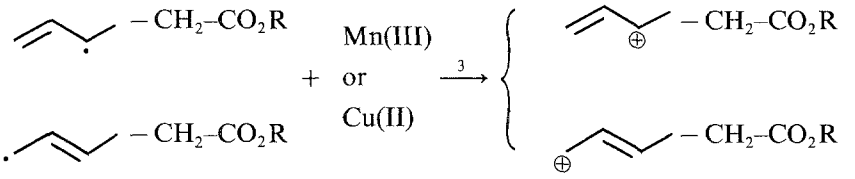

Up to this point the mechanism is the same whether R in CH_3–CO_2R is H (for acetic acid) or Ac (for acetic anhydride).

If R is H then lactone is the major product.

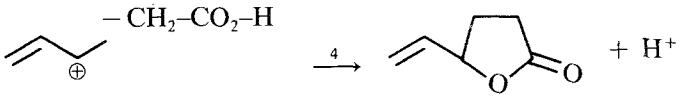

If R is $-\overset{O}{\overset{\|}{C}}-CH_3$ then acetoxyhexenoic acids are the major products.

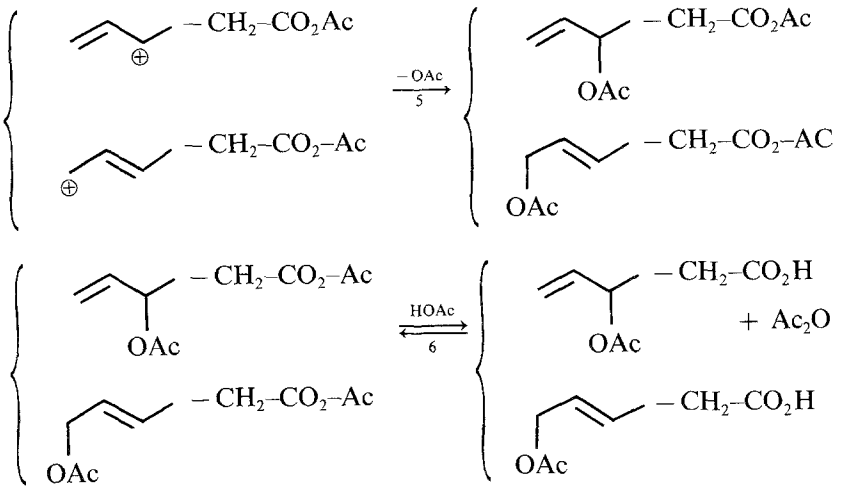

The equilibrium in step 6 is probably very much towards the right hand side, since acetoxyhexenoic acids were the primary products found. Note that in the formation of 1 mole of AA, 2 moles of Mn(III) are consumed as well as 1 mole of acetic acid and 1 mole of butadiene. There is no net consumption of acetic anhydride: it is used in step 1 but is formed back in step 6.

Possible side reactions are the formation of acetoxyacetic acid and oligomers and further reaction between Mn(III) and the products. Mn(III) reacts with AA probably in a similar fashion as it does with acetic acid.

4.2. *Reaction modelling*

The electrochemical synthesis of acetoxyhexenoic acids involves both electrochemical and chemical reactions. As can be seen from the mechanism section, the chemical reactions themselves are already rather complex to be fully modelled, let alone taking into account possible interactions between the two. Under normal electrolysis conditions, however, only a few reaction steps seem to be dominating, allowing the system to be adequately described by the following simple three-step model.

Since the amount of lactone formed as a by-product is rather small under typical electrochemical experiments, lactone formation will be lumped into AA in this model. Both solution kinetic studies and electrolysis results suggest that the rate-determining step for AA formation is the reaction between Mn(III) and acetic anhydride. As long as it is present in sufficient amounts, butadiene does not seem to affect the rate. The following three-step model is proposed.
At the anode:

$$\mathrm{Mn(II)} \xrightarrow{\text{current}} \mathrm{Mn(III)} \tag{1}$$

In solution:

$$2\mathrm{Mn(III)} + \mathrm{Ac_2O} \xrightarrow[\substack{\mathrm{Cu(II)}\\ \mathrm{HOAc}}]{} \mathrm{AA} + \mathrm{Ac_2O} + 2\mathrm{Mn(II)} \tag{2}$$

$$\mathrm{Mn(III)} + \mathrm{AA} \longrightarrow \text{High boilers} \tag{3}$$

Note that in step 2 acetic anhydride (Ac_2O) is involved in the reaction but is not consumed. First, the rate equations describing those three steps are needed.

The rate of Mn(III) generation from step 1 depends on the current input only, assuming the current efficiency for the oxidation of Mn(II) to Mn(III) is 100%.

$$r_{\text{gen}} = \frac{I}{F} \times 60 \text{ mol Mn(III) min}^{-1}$$

where I is the current input (A) and F is the Faraday constant. The rate of Mn(III) consumed by step 2 is given by

$$r_2 = k_2(\mathrm{Mn^{3+}})(\mathrm{Ac_2O}) = 2 \times \text{rate of AA formation}$$

where k_2 is a function of butadiene concentration and Cu(II) as well as temperature. The first order with respect to Mn(III) and Ac_2O is consistent with solution kinetics. The factor 2 accounts for 2 moles of Mn(III) being consumed for 1 mole of AA.

The rate of AA consumed by step 3 is given by

$$r_3 = k_3(\mathrm{Mn^{3+}})(\mathrm{AA})$$

The first order for Mn(III) and AA is also consistent with solution kinetics.

It has been shown that the continuous electrolysis unit as a whole behaves very much like a constant stirred tank reactor (CSTR). For this type of reactor, the mass balance for Mn^{3+} is given by

$$V\frac{\mathrm{d[Mn^{3+}]}}{\mathrm{d}t} = r_{\text{gen}} - Vk_2[\mathrm{Mn^{3+}}][\mathrm{Ac_2O}] - Vk_3[\mathrm{Mn^{3+}}][\mathrm{AA}] - N[\mathrm{Mn^{3+}}] \tag{4}$$

The mass balance for AA is given by

$$V\frac{\mathrm{d[AA]}}{\mathrm{d}t} = \frac{Vk_2[\mathrm{Mn^{3+}}][\mathrm{Ac_2O}]}{2} - Vk_3[\mathrm{Mn^{3+}}][\mathrm{AA}] - N[\mathrm{AA}] \tag{5}$$

where N is the liquid feed rate ($1\,\mathrm{min}^{-1}$) and V is the volume of anode compartment + reactor (l).

At the steady state there is no change in concentration:

$$\frac{\mathrm{d[Mn^{3+}]}}{\mathrm{d}t} = \frac{\mathrm{d[AA]}}{\mathrm{d}t} = 0 \tag{6}$$

Manipulating Equations 4–6 leads to the following explicit expressions for k_2 and k_3:

$$k_2 = \frac{r_{gen} + N([AA] - [Mn^{3+}])}{1.5[Ac_2O][Mn^{3+}]V} \quad (7)$$

$$k_3 = \frac{r_{gen} - N(2[AA] - [Mn^{3+}])}{3[AA][Mn^{3+}]V} \quad (8)$$

Thus, from the steady-state data of a single continuous run the values of k_2 and k_3 can be calculated since V, N, I, [AA] and [Mn^{3+}] are known. With k_2 and k_3 known, Equations 4–6 can be used to calculate the steady-state concentrations of Mn^{3+} and AA for other values of feed rate, current and acetic anhydride concentration. The effects of these parameters on the system performance can therefore be simulated.

Fig. 8 shows the comparison between the experimental data and the model prediction for AA current efficiency as a function of AA payload. As can be seen, the agreement is quite remarkable for this rather simple model. There is some deviation at high payloads but the difference is probably within experimental errors.

With k_2 and k_3 known, the two differential Equations 4 and 5 can be integrated numerically to simulate the transient period that the system experiences before it reaches steady state. Transient data are valuable in the sense that they provide information not normally available from steady-state data. Fig. 6 shows transient data for AA and Mn^{3+} and the corresponding model predictions. The prediction follows the rise in AA concentration reasonably well, which is rather pleasing considering the fact that no adjustable parameters are involved. The prediction for Mn^{3+} concentration, however, shows a rather low maximum compared to the data. It looks as if the Mn(III)–Ac_2O reaction initially underwent an induction period (complex formation?), allowing Mn(III) concentration to rise higher than would be predicted from steady-state rates. This induction phenomenon, if exists, is not likely to affect the steady-state behaviour.

The proposed model is thus quite sufficient for describing our electrochemical reaction system within or near the range of experimental conditions studied. A more complex reaction model that takes into account practically all the possible reaction steps and is therefore more general has also been worked out qualitatively.

Acknowledgements

The author wishes to thank the Monsanto Corporate Research Electrochemistry Group for their valuable input regarding the electrochemical aspects of this work, S. R. Auvil for his help in the conceptual design of the experimental set-up, and J. R. Smith for his excellent assistance in carrying out the experimental work.

References

[1] R. Clarke, A. T. Kuhn and E. Okoh, *Chem. in Brit.* **11** (2) (1975) 59.
[2] K. Kramer, P. M. Robertson and N. Ibl, *J. Appl. Electrochem.* **10** (1980) 29.
[3] Fr. Fichter, 'Organische Elektrochemie', Steinkopff, Leipzig (1942). (Reissued Salford University Bookshop, 1970, p. 75 *et seq.*)
[4] US Patent 4 022 822 (1977).
[5] US Patent 4 158 741 (1979).
[6] J. H. Wagenknecht, J. P. Coleman, R. C. Hallcher, D. E. McMackins, T. E. Rogers and W. G. Wagner, *J. Appl. Electrochem.* **13** (1983) 535.
[7] R. E. van der Ploeg, R. W. de Korte and E. C. Kooyman, *J. Catal.* **10** (1968) 52.
[8] L. W. Hessel, Thesis, Leiden, The Netherlands (1968).
[9] E. I. Heiba, R. M. Dessau and W. J. Koehl, Jr., *J. Amer. Chem. Soc.* **90** (1968) 5905.
[10] W. J. Klein, *Rec. Tran. Ann.* **96** (1977) 22.
[11] J. B. Bush, Jr. and Herman Finkbeiner, *J. Amer. Chem. Soc.* **90** (1968) 5905.
[12] W. J. Klein, *Rec. Tran. Ann.* **94** (1975) 48.